Synthesis and Characterization of forsterite nanopowder ceramic via mechanical activation

Hassan Gheisari Dehsheikh

Biomaterials Dep, University of Toronto AND University of Najafabad,Isfahan,Iran

ARTICLE INFO

ABSTRACT

This project investigates the synthesis of single-phase nano crystalline forsterite powder by mechanical activation with subsequent annealing. To produce forsterite powder, a mixture of talc and magnesium oxide powders was first milled by a planetary ball mill, and then annealed at 1000 and 1200 8C for 1 h. The synthesized powder was characterized by X-ray diffraction (XRD), simultaneous thermal analysis (STA), scanning electron microscopy (SEM), and atomic absorption spectrometry (AAS). The initial temperature of forsterite crystallization was reduced to about 825 8C after 20 h of mechanical activation. The forsterite powder synthesized by 5 h of mechanical activation with subsequent annealing at 1000 8C for 1 h had crystallites 40 n min size. The particle size of this sample was less than 500 nm.

How to cite this article

INTRODUCTION

Forsterite, named after the German naturalist Johann Forster, is a crystalline magnesium silicate belonging to the group of olivine with the chemical formula Mg_2SiO_4. Forsterite has an extremely low electrical conductivity [1]. This makes forsterite ceramics an ideal material for tunable laser [2]. Furthermore, forsterite shows good refractoriness, with a melting point of 1890 8C, low thermal expansion, chemical stability, and excellent insulation properties even at high temperatures. The manufacturers of the SOFC (solid oxide fuel cells) find forsterite interesting due to its linear thermal expansion coefficient, perfectly matching the other cell components, and also for its very high stability in fuel cell environments [3,4]. Its precursor powders and xerogels have been synthesized via the sol–gel method [5–9]. The methods commonly used for preparing forsterite include heating MgO and SiO_2 powders (up to 1525 8C) [10], co-precipitation [11], molten-salt approach [12], polymer precursor method [13], and the synthetic route comprising the heating of Au-coated Si substrates with simultaneous evaporation of MgO [14]. Although fabrication of forsterite by mechanical activation and thermal treatment has also been investigated [3,15] producing pure nanocrystalline forsterite has not yet been reported. The main point in synthesizing forsterite ceramics involves provisions to avoid the appearance of $MgSiO_3$ and MgO secondary phases. As pure forsterite is hard to produce, the present work aim to develop a novel, simple, and economical method for the synthesis of single-phase nanocrystalline forsterite powder from talc ($Mg_3Si_4O_{10}(OH)_2$) and magnesium oxide (MgO).

EXPERIMENTAL PROCEDURE

Preparation of forsterite powder

In this study, talc ($Mg_3Si_4O_{10}(OH)_2$) (98% purity, Merck) and periclase (MgO) (98% purity, Merck) were used as initial, starting powders. To obtain the forsterite single phase,

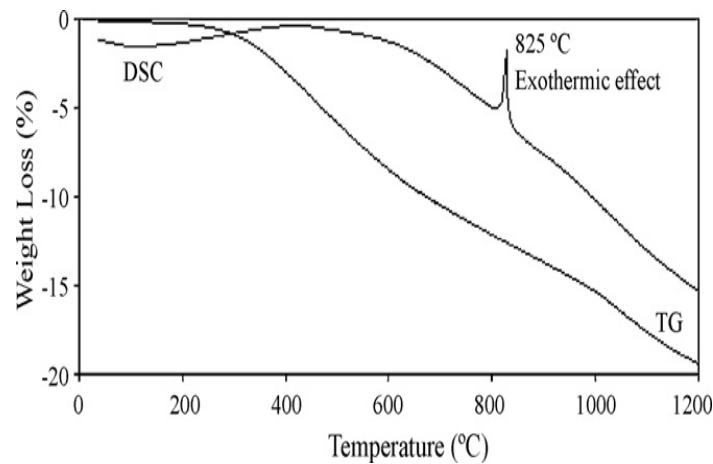* Corresponding Author Email: *hassan.gh.d@gmail.com*

Fig. 1. TG and DSC traces of powder obtained after 20 h of mechanical activation.

MgO and talc powders at a molar ratio of 5 were mixed and as much as 16.5 g

of the mixture was then mechanically activated in a planetary ball mill (Fritsch P7 type) under ambient conditions. The milling

media consisted of a hardened steel vial (125 ml) with five 20 mm steel balls. In all milling runs, the ball-to-powder weight

ratio was approximately 10:1 and the rotational speed of the main disc was set at 500 rpm. The maximum milling time was

60 h and annealing was carried out at 1000 and 1200 8C for 1 h in the air.

Characterization of forsterite powder

The powders were characterized by X-ray diffraction (XRD), scanning electron microscopy (SEM), simultaneous thermal analysis (STA), and thermogravimetric analysis (TG). XRD was performed in a Philips X'PERT MPD diffractometer (Cu Ka radiation: μ = 0.154056 nm at 20 kV and 30 mA). The XRD patterns were recorded in the 2θ range of 20–808 (step size 0.048 and time per step 1 s). The apparent crystallite sizes of the powders were determined using the Williamson–Hall's equation [15]:

$$ß\,Cos\theta = \frac{0.9\mu}{t} + Sin\theta \qquad (1)$$

where t is grain size; μ, wavelength (μ = 0.154056 nm); ß, peak width in the middle of its height; u, the Bragg's angle; and e is residual strain in powder. A PerkinElmer atomic

absorption spectrometer (Model 2380) was used for determination of iron and chromium contamination introduced in the 60 h milled sample. SEM was performed in a Philips XL30 at an accelerating voltage of 30 kV. The image analysis method was used to measure forsterite powder particles. STA was performed on as-milled powders to observe any exothermic peaks, which may indicate crystallization temperatures of forsterite. To evaluate the weight loss of the milled powder during subsequent heating, the thermogravimetry (TG) test was performed for up to 1200 8C under nitrogen gas flow and at a heating rate of 10 8 C/min.

RESULTS AND DISCUSSION

Fig. 1 shows TG and DSC traces of powder after 20 h of ball milling. As can be seen, contiguous weight loss occurred from room temperature to as high as 1200 8C, possibly due to the loss of hydration water of MgO and also liberation of the talc's structural water [14]. DSC trace exhibited a distinct exothermic peak at 825 8C, which can be attributed to the formation of forsterite structure [11]. No other significant endothermic and/or exothermic peaks were observed. So, annealing above 825 8C was performed in order to prepare the single-phase forsterite.

XRD phase analysis

Fig. 2 shows the XRD patterns of powders after different mechanical activation times. The XRD patterns of initial powders after 5 min of
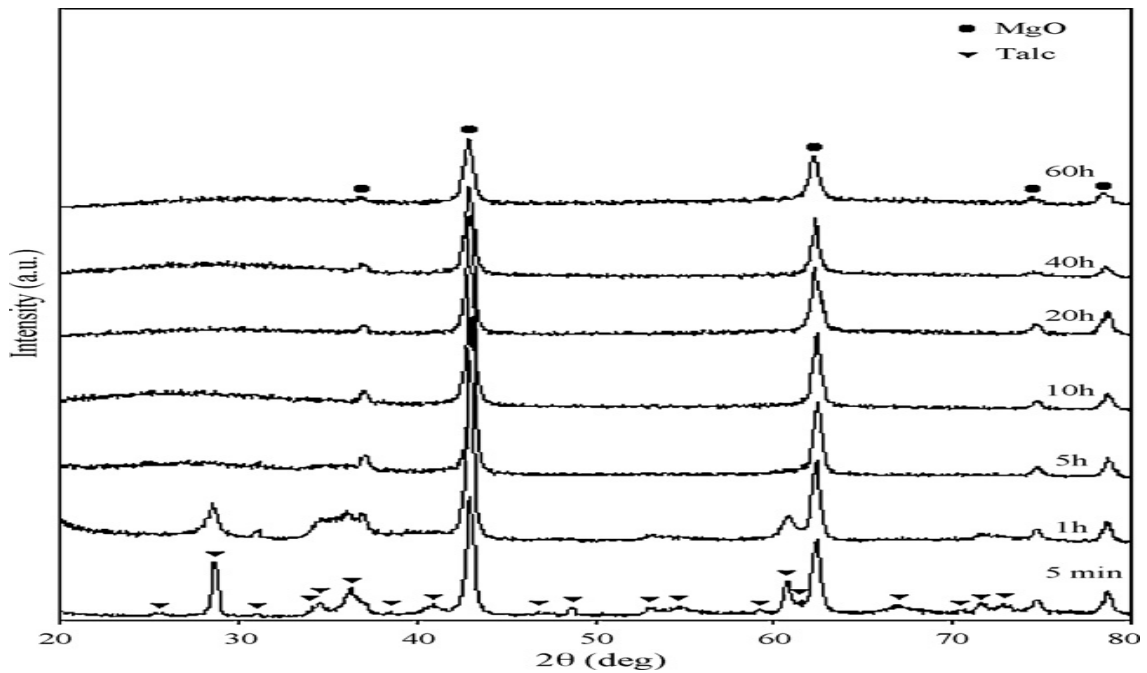
Fig. 2. X-ray diffraction patterns of starting materials after mechanical activation for various periods of time.

mechanical activation corresponded to those of talc (XRD JCPDS data file No. 13-0558) and MgO (XRD JCPDS data file No. 43-1022) phases. After milling for 5 h, talc peaks disappeared. This means that milling gradually drives talc into an amorphous state. But MgO peaks still persisted even after 60 h of milling. An increase in milling time by up to 60 h led to the broadening of XRD peaks and a significant decrease in their intensity as a result of refinement of crystallite size and to an enhancement of the lattice strain. No new crystalline phase was observed in the XRD patterns. To check for the possible formation of the forsterite phase during subsequent heat treatment, the milled powders were annealed at 1000 and 1200 8C for 1 h. Fig. 3a shows the structure of the samples after annealing at 1000 8C. As shown in Fig. 3a, for the sample milled for 5 min, annealing led to complete vanishing of the talc. Additionally, the periclase peaks with strong intensity appeared in the XRD pattern. Traces of enstatite (XRD JCPDS data file No. 11- 0273) and forsterite (XRD JCPDS data file No. 34-0189) could also be observed in this stage. According to Eq. (2), it seems that at the initial stage, the talc must have reacted with MgO to produce enstatite (MgSiO3).

Mg3Si4O10(OH)2⌐+ MgO=>4MgSiO3+H2O

ΔG1000_ C =147.333 kJ/mol K

After this stage, the produced enstatite reacted with the remaining MgO according to Eq. (3):

MgO +MgSiO3=> Mg2SiO4 , ΔG1000° C = -21.856 kJ/mol K   (3)
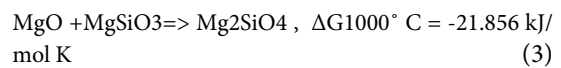
The negative value of ΔG1000 C in reaction (3) suggests that this reaction could have taken place thermodynamically. The value of ΔH1000 C in reaction (3) is also negative (-30.599 kJ/mol K), indicating that this reaction is exothermic. The adiabatic temperature, Tad, was calculated for reaction (3) and found to be 220 8C, suggesting that the formation of forsterite occurs in a slow diffusional process rather than in a rapid combustion reaction. This finding agrees with those reported by Brindley and Hayami [7] who studied the reaction of MgO and SiO2. They proposed that MgO initially reacts at the surface of the SiO2 to form enstatite, followed by the diffusion of MgO takes place through the enstatite layer, forming the forsterite phase. In the case of the sample milled for 5 h, the peaks of periclase as well as enstatite disappeared after annealing. Fast disappearance of MgO diffraction peaks is the result of the milling effect on reaction rate. After milling for 10 h, the peaks of periclase (2θ ~ 43°) reappeared and
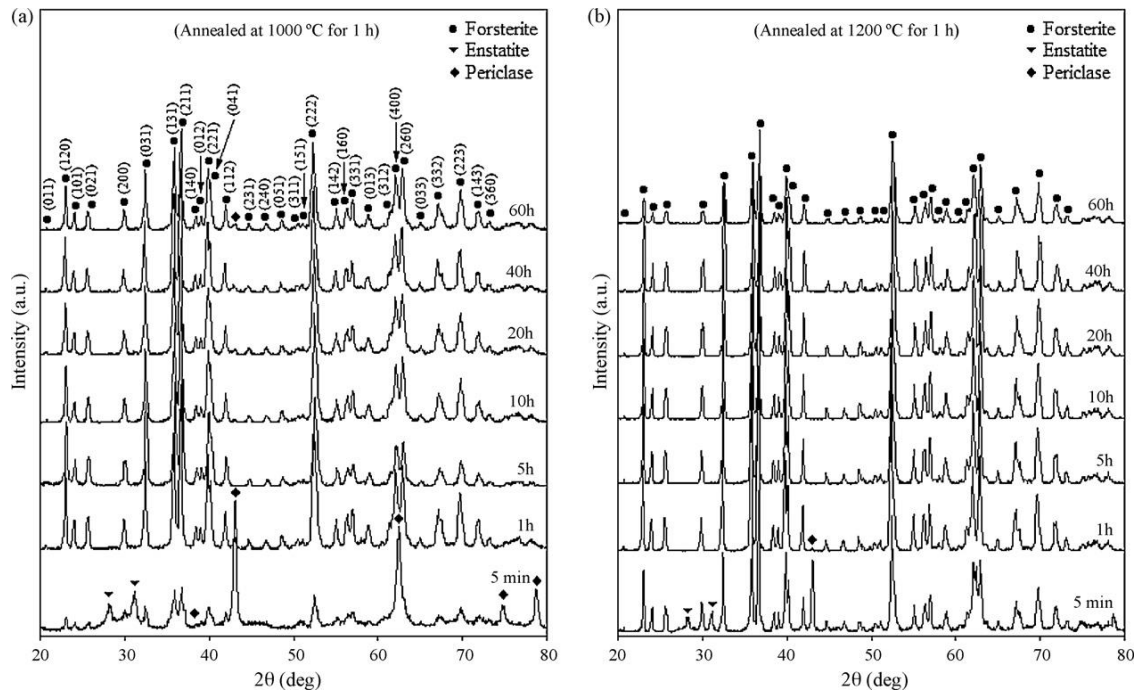
Fig. 3. X-ray diffraction patterns of starting materials after different mechanical activation times and then (a) annealed at 1000 8C for 1 h and (b) annealed at 1200 8C for 1 h.

persisted until 60 h of mechanical activation had been accomplished after annealing. This indicates that some imperceptible MgSiO3 must have remained in the sample for the stoichiometry ratio of 2:1 for Mg:Si in the forsterite.

This situation is frequently encountered in the synthesis of forsterite. Even after heating up to 1540 8C for 5 h, which is close to the melting point of enstatite, MgSiO3 and MgO had not completely reacted to form Mg2SiO4 [4]. Fig. 3b shows the structure of the samples after annealing at 1200 8C for 1 h. As can be seen in Fig. 3b, the fraction of the forsterite phase increased with increasing milling time while the periclase and enstatite contents reduced after annealing, so that, only the forsterite phase was detectable in the sample milled for 5 h. Further milling up to 60 h had no significant effects on the structure or phase composition of the samples after subsequent annealing. The interface area of reacting phases increases as a result of mechanical activation which, in turn, improves the reaction kinetics during subsequent annealing. The absence of periclase and enstatite on XRD patterns indicates that during mechanical activation, a homogeneous powder mixture was

achieved. This result is opposed to those from previous studies that reported the formation of periclase and enstatite phases in the final product due to lack of homogeneity of reactants [4,15]. The crystallite size of the forsterite powder, which was fabricated by mechanical activation with subsequent annealing at 1000 and 1200 8C, can be determined by Williamson–Hall equation [13]. The crystallite size of the forsterite powder prepared by 5 h of mechanical activation with subsequent annealing at 1000 8C was 40 nm. The crystallite size of the forsterite powder obtained through of 5 h of mechanical activation and 1 h of annealing at 1200 8C decreased from 138 nm to 33 after 60 h of mechanical activation and subsequent annealing at 1200 8C.

AAS analysis

Fe and Cr contaminations from the wear of milling media are too small to be detected by XRD. Atomic absorption spectrometry (AAS) was used to measure Fe and Cr contaminations. AAS analysis confirmed the low contamination levels of Fe and Cr in powder particles, which were 0.4256% and 0.00365 wt.%, respectively, in the sample ball milled
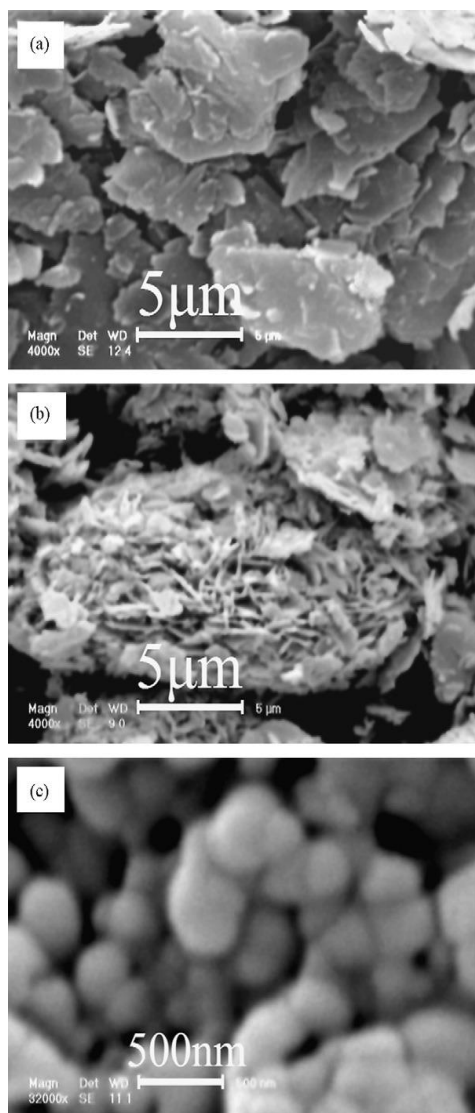
Fig. 4. SEM micrograph of starting materials including: (a) talc, (b) MgO, and (c) prepared forsterite powder after 60 h of mechanical activation with subsequent annealed at 1200 8C for 1 h.

for 60 h. This slight amount of contamination can have no significant effects on the properties of the final product.

SEM evaluation

The SEM micrographs of the initial powders and single-phase nanocrystalline forsterite powder prepared by 60 h of mechanical activation with subsequent annealing at 1200 8C are shown in Fig. 4. The talc powder had a lamellar shape with a mean particle size of about 20 mm (Fig. 4a). The MgO powder was needle-shaped with a mean

particle diameter of about 5 mm (Fig. 4b). Several micrographs were used to measure particle size and the average value was reported. As can be seen in Fig. 4c, the forsterite powder synthesized by 60 h of mechanical activation with subsequent annealing at 1200 8C enjoyed a uniform distribution of particle size that was less than 500 nm.

CONCLUSION

The present work is a novel effort to produce pure nanocrystalline forsterite powder from talc. Mechanical activation plays the main role in producing the pure single-phase nanocrystalline forsterite powder which is synthesized by mechanical activation of talc and magnesium oxide for 5 h with subsequent annealing at 1000 8C for 1 h. The crystallite size of the sample obtained was 40 nm, and its particle size was submicron. The powder can equally be obtained through 20–60 h of mechanical activation with subsequent annealing at 1200 8C for 1 h, which is useful for the construction of bulk samples where higher sintering temperatures are required. AAS analysis showed that the amount of Fe and Cr in the sample ball milled for 60 h were 0.4256% and 0.00365%, respectively.

CONFLICT OF INTEREST

The authors declare that they have no conflict of interest.

REFERENCES

1. Con TH, Loan DK. Preparation of silver nano-particles and use as a material for water sterilization. Environment Asia, 2011; 4(1): 62-66.

2. Lu HW, Liu SH, Wang XL, Qian XF, Yin J, Zhu ZK. Silver nanocrystals by hyperbranched polyurethane-assisted photochemical reduction of Ag+. Materials Chemistry and Physics. 2003;81(1):104-7.

3. Gheisari H, Karamian E, Abdellahi M. A novel hydroxyapatite –Hardystonite nanocomposite ceramic. Ceramics International. 2015;41(4):5967-75.

4. H.Gheisari and E.Karamian , Preparation and characterization of hydroxyapatite reinforced with hardystonite as a novel bio-nanocomposite for tissue engineering ,2014;1(2):298-301

5. N.Y. Iwata, G.H. Lee, Y. Tokuoka, N. Kawashima, Colloids Surf B interfaces. 2004;3(1); 239–245.

6. Karamian E, Abdellahi M, Gheisari H. Fluorine-substituted HA reinforced with zircon as a novel nano-biocomposite ceramic: Preparation and characterization. International Journal of Materials Research. 2015;106(12):1285-90.

7. Gheisari Dehsheikh H, Ghasemi-Kahrizsangi S. Performance improvement of MgO-C refractory bricks by the addition of Nano-ZrSiO 4. Materials Chemistry and Physics. 2017;202:369-76.

8. Ghasemi-Kahrizsangi S, Dehsheikh HG, Karamian E. Impact of Titania nanoparticles addition on the microstructure and properties of MgO-C refractories. Ceramics International. 2017;43(17):15472-7.

9. Ghasemi-Kahrizsangi S, Gheisari Dehsheikh H, Boroujerdnia M. Effect of micro and nano-Al 2 O 3 addition on the microstructure and properties of MgO-C refractory ceramic composite. Materials Chemistry and Physics. 2017;189:230-6.

10. Bag M, Adak S, Sarkar R. Study on low carbon containing MgO-C refractory: Use of nano carbon. Ceramics International. 2012;38(3):2339-46.

11. Bag M, Adak S, Sarkar R. Nano carbon containing MgO-C refractory: Effect of graphite content. Ceramics International. 2012;38(6):4909-14.

12. Salman Ghasemi-Kahrizsangi, Ebrahim Karamian, Hassan Gheisari Dehsheikh, Ahmad Ghasemi-Kahrizsangi, "A Review on Recent Advances on Magnesia-Doloma Refractories by Nano-Technology", Journal of Water and Environmental Nanotechnology, 2017;3(2):206-222.

13. Salman Ghasemi-Kahrizsangi, Hassan Gheisari Dehsheikh, Ebrahim Karamian, Mehdi Boroujerdnia, Khoshnaz Payandeh "Effect of MgAl2O4 nanoparticles addition on the densification and properties of MgO-CaO refractories", Ceramics International, 2017;6(2): 5014-5019

14. Ghasemi-Kahrizsangi S, Barati Sedeh M, Gheisari Dehsheikh H, Shahraki A, Farooghi M. Densification and properties of ZrO2 nanoparticles added magnesia–doloma refractories. Ceramics International. 2016;42(14):15658-63.

15. M. Boroujerdnia S. Ghasemi-kahrizsangi, H. Gheisari-dehsheikh, "the effect of nano meter size ZrO2 particles addition on the densification and hydration resistance of magnesite– dolomite refractories", Iranian Journal of Materials Science and Engineering, 2016;4(1): 33-40.